of England: molecular characterisation of a genetically distinct isolate. J. Med. Virol. **67**:282–288.
26. **Schuffenecker, I., T. Ando, D. Thouvenot, B. Lina, and M. Aymard.** 2001. Genetic classification of "Sapporo-like viruses." Arch. Virol. **146**:2115–2132.
27. **Seah, E. L., J. A. Marshall, and P. J. Wright.** 1999. Open reading frame 1 of the Norwalk-like virus Camberwell: completion of sequence and expression in mammalian cells. J. Virol. **73**:10531–10535.
28. **Smiley, J. R., K. O. Chang, J. Hayes, J. Vinjé, and L. J. Saif.** 2002. Characterization of an enteropathogenic bovine calicivirus representing a potentially new calicivirus genus. J. Virol. **76**:10089–10098.
29. **Someya, Y., N. Takeda, and T. Miyamura.** 2000. Complete nucleotide sequence of the Chiba virus genome and functional expression of the 3C-like protease in Escherichia coli. Virology **278**:490–500.
30. **Someya, Y., N. Takeda, and T. Miyamura.** 2002. Identification of active-site amino acid residues in the Chiba virus 3C-like protease. J. Virol. **76**:5949–5958.
31. **Sosnovtsev, S. V., M. Garfield, and K. Y. Green.** 2002. Processing map and essential cleavage sites of the nonstructural polyprotein encoded by ORF1 of the feline calicivirus genome. J. Virol. **76**:7060–7072.
32. **Sosnovtseva, S. A., S. V. Sosnovtsev, and K. Y. Green.** 1999. Mapping of the feline calicivirus proteinase responsible for autocatalytic processing of the nonstructural polyprotein and identification of a stable proteinase-polymerase precursor protein. J. Virol. **73**:6626–6633.
33. **Vinjé, J., H. Deijl, R. van der Heide, D. Lewis, K.-O. Hedlund, L. Svensson, and M. P. G. Koopmans.** 2000. Molecular detection and epidemiology of Sapporo-like viruses. J. Clin. Microbiol. **38**:530–536.
34. **Wei, L., J. S. Huhn, A. Mory, H. B. Pathak, S. V. Sosnovtsev, K. Y. Green, and C. E. Cameron.** 2001. Proteinase-polymerase precursor as the active form of feline calicivirus RNA-dependent RNA polymerase. J. Virol. **75**:1211–1219.
35. **Wirblich, C., M. Sibilia, M. B. Boniotti, C. Rossi, H.-J. Thiel, and G. Meyers.** 1995. 3C-like protease of rabbit hemorrhagic disease virus: identification of cleavage sites in the ORF1 polyprotein and analysis of cleavage specificity. J. Virol. **69**:7159–7168.
36. **Wirblich, C., H. J. Thiel, and G. Meyers.** 1996. Genetic map of the calicivirus rabbit hemorrhagic disease virus as deduced from in vitro translation studies. J. Virol. **70**:7974–7983.

Arch Virol (2005) 150: 2529–2538
DOI 10.1007/s00705-005-0599-5

Archives of Virology
Printed in Austria

Deletion analysis of the sapovirus VP1 gene for the assembly of virus-like particles

G. S. Hansman, N. Matsubara, T. Oka, S. Ogawa, K. Natori, N. Takeda, and **K. Katayama**

Department of Virology II, National Institute of Infectious Diseases, Tokyo, Japan

Received February 1, 2005; accepted May 19, 2005
Published online August 1, 2005

Summary. Human sapovirus (SaV) strains are agents of gastroenteritis. They cannot be grown in cell culture. In this study, constructs containing SaV N- and C-terminal-deleted recombinant capsid proteins (rVP1) were expressed in a baculovirus expression system to allow us to better understand the sequence requirements for the formation of virus-like particles (VLPs). Only proteins derived from N-terminal-deleted rVP1 constructs that began 49 nucleotides downstream assembled into VLPs, which included both small and native-size VLPs. Our results were similar to those reported in a rabbit hemorrhagic disease virus (RHDV) N- and C-terminal-deleted rVP1 expression study but were distinct from those reported in a norovirus N- and C-terminal-deleted rVP1 expression study, suggesting that SaV and RHDV may have similar expression requirements.

Introduction

The family *Caliciviridae* contains four genera, *Sapovirus*, *Norovirus*, *Lagovirus*, and *Vesivirus*, which include sapovirus (SaV), norovirus (NoV), rabbit hemorrhagic disease virus (RHDV), and feline calicivirus (FCV) strains, respectively. Despite the fact that strains from these four genera are genetically and antigenically distinct, some characteristics are common. For example, the major capsid gene of SaV and RHDV is fused to the non-structural genes on open reading frame 1 (ORF1), whereas the major capsid gene of NoV and FCV is located on a separate ORF (ORF2). This suggests that SaV/ RHDV and NoV/ FCV have similar proteolytic processing or expression characteristics, respectively.

SaV strains can be divided into five genogroups (GI-GV), of which GI, GII, GIV, and GV strains infect humans, while GIII strains infect porcine species. The SaV GI, GIV, and GV genomes are predicted to each contain three main ORFs,

whereas the SaV GII and GIII genomes each have only two main ORFs. SaV ORF2 and ORF3 encode proteins of yet-unknown functions. Human SaV strains are noncultivable, but expression of the SaV recombinant capsid protein (rVP1) in a baculovirus expression system results in the self-assembly of virus-like particles (VLPs) that are morphologically similar to native SaV [10]. Recently, cryo-EM analysis of SaV VLPs and X-ray crystallography analysis of NoV VLPs predicted the SaV shell (S) and protruding (P) domains that were based the NoV domains [5, 11]. NoV N and C-terminal rVP1 deletion analysis showed that the S domain controlled the assembly of the VLPs (i.e., N-terminal residues 1–225), whereas the P domain (residues beyond 226) controlled the size and stability of the VLPs [2].

Since human caliciviruses are uncultivable, determination of their antigenic characteristics and proteolytic processing has mostly relied on expression in bacterial or insect cells. In a previous study, we compared the time-course expression of two different full-length SaV (Mc114 strain, GenBank accession number AY237422) rVP1 in a baculovirus expression system [9]. One construct had the

Constructs		Western blot (antisera)			EM (nm)	Expected rVP1 size
		VLP	N-term	C-term		
Wt	1 VP1 VP2	+	+	+	41-48	60K
MQG-1076	1 * *	+	+	+	41-48	60K
NT49-Wt	49	+	+	+	21-31 and 41-48	58K
NT49-MQG-1076	49 *	+	+	+	21-31 and 41-48	58K
NT143-Wt	143	+	-	+	-	55K
NT143-MQG-1076	143 *	-	-	+	-	55K
CT1583-MQG-1076	1 1583 * *	-	+	+	-	56K
CT1260-MQG-1076	1 1260 * *	+	+	+	-	44K
CT1068-MQG-1076	1 1068 * *	+	+	+	-	38K
CT687-MQG-1076	1 687 * *	+	+	-	-	24K

Fig. 1. The schematic of the rVP1 constructs and predicted sizes, and the results of the Western blot and EM analysis. All constructs were amplified with the specific sense primer and an identical antisense primer, attB2TX30SXN, and included the ORF2 and poly(A) sequences. The N-terminal constructs began downstream from the predicted start codon (49 or 143 nt). The asterisks represent the nucleotide mutations that resulted in amino acid substitutions. The C-terminal constructs began from the predicted start and were identical to the MQG-1076 construct except for the introduced stop codons, as indicated by the dashed line and the corresponding number above

native sequence (Wt construct), whereas the other (MQG-1076 construct) had two nucleotide point mutations in VP1 at positions 4 and 1076 (relative to VP1 start) resulting in two amino acid substitutions, one at the second residue where glutamic acid (E) → glutamine (Q), and one at residue 358 where asparagine (N) → serine (S) (Fig. 1). A silent nucleotide point mutation in VP2 also occurred in the MQG-1076 construct at position 1895 (relative to VP1 start). These mutations were probably introduced by PCR errors. While both constructs formed VLPs, the MQG-1076 construct had increased yields of VLPs.

In the current study, we expressed N- and C-terminal-deleted Mc114 rVP1 constructs in a baculovirus expression system to determine the sequence requirements for expression of rVP1 and assembly of VLPs.

Materials and methods

PCR, sequencing, electron microscopy (EM), and Western blotting were performed as previously described [10]. For this study, all constructs were amplified with a specific sense primer and the same antisense primer, attB2TX30SXN, and included the ORF2 (VP2) and poly(A) sequences. The primers listed in Table 1 were used to re-amplify the inserted VP1 sequence from the pDEST8-Wt and pDEST8-MQG-1076 plasmids, which were then cloned into a new pDONR201 vector (Invitrogen, Carlsberg, CA, USA). The NT49 constructs were designed to start from a second inframe methionine downstream from the predicted VP1 start, whereas for the NT143 constructs, we introduced an inframe methionine. Four N-terminal-deleted rVP1 constructs were designed. Two contained the Wt construct sequence (NT49-Wt and NT143-Wt), and two contained the MQG-1076 construct sequence (NT49-MQG-1076 and NT143-MQG-1076), i.e., nucleotide mutations at 1076 and 1895 (Fig. 1).

Since the MQG-1076 construct had increased yields of VLPs, we used this construct as the template for all C-terminal-deleted rVP1 constructs (CT1583-MQG-1076, CT1260-MQG-1076, CT1068-MQG-1076, and CT687-MQG-1076) in which we introduced an inframe stop codon to retain RNA stability [3]. Briefly, two sets of sense and antisense primers were used in separate PCR to create two overlapping PCR fragments. For the CT687-MQG-1076 construct, primers CT-F and CT687-R were used for the first PCR, and then primers CT-687-F and CT-R were used for the second PCR. These two purified fragments were used as templates in a primer-less PCR, with the results then amplified with CT-F and CT-R primers, creating a single PCR fragment with two internal introduced stop codons. Restriction enzymes *Cla*I and *Eco*RI were used to cut the single PCR fragment (corresponding to nucleotides 352–357 and 1613–1616 on the VP1 gene, respectively), which was then ligated into a previously *Cla*I- and *Eco*RI-digested pDEST8-MQG-1076 plasmid. CT1260-MQG-1076, CT1068-MQG-1076, and CT1583-MQG-1076 constructs were produced in a similar way except for the primers.

All plasmids were confirmed by sequencing. Expression was then carried out as previously described [10]. Briefly, recombinant bacmids were transfected into Sf9 cells (Riken Cell Bank, Japan). The purified recombinant baculoviruses were used to infect Tn5 cells (Invitrogen) at a multiplicity of infection of 5–10 in 1.5 ml of Ex-Cell 405 medium (JRH Biosciences, USA), and the infected cells were incubated at 26 °C. The culture medium was harvested 5–6 days post-infection (dpi), centrifuged for 10 min at 3,000 × *g*, and further centrifuged for 30 min at 10,000 × *g*. The VLPs were concentrated by ultracentrifugation for 2 h at 45,000 rpm at 4 °C (Beckman TLA-55 rotor) and then resuspended in 30 µl of Grace's medium. Samples were examined for VLP formation by electron microscopy (EM).

To collect RNA, we harvested the insect cells at 2 dpi, dissolved them with 1 ml of Isogen-LS, and purified them following the manufacturer's instructions (Nippon Gene, Tokyo,

Table 1. Names, sequences, nucleotide positions, and polarity of the primers used in this study

Primer	Sequence (5′ to 3′)	Position (nt)	Sense	Construct generated
TX30SXN	GACTAGTTCTAGATCGCGAGCGGCCGCCCTTTTTTTTTTTTTT TTTTTTTTTTTTTTT	End	−	
Wt	GGGGACAAGTTTGTACAAAAAAGCAGGCTTCGAAGGAGATA GAACCATGGAGGGCAATGGCTCCAACTCAGAGCCAAAG	1–33	+	Wt
NT49	GGGGACAAGTTTGTACAAAAAAGCAGGCTTCGAAGGAGATA GAACCATGGTCGTTGACCCGCCTGGCACAACAGGTCCG	49–81	+	NT49-Wt and NT49-MQG-1076
NT143	GGGGACAAGTTTGTACAAAAAAGCAGGCTTCGAAGGAGAT AGAACCatGTTGGCTGTTGCCACTGGTGCAATCCAATCCA	145–176	+	NT143-Wt and NT143-MQG-1076
CT687-F	AGGCCACCAGGTCAACAGtaGtAAAATGGGGTTTCACCAGAAG	670–712	+	CT687-MQG-1076
CT687-R	CTTCTGGTGAAACCCCATTTTaCtaCTGTTGACCTGGTGGCCT		−	
CT1068-F	GCCTGCCATAAGCTTCtAAtAgAATGGTGATGTGTACGAA	1053–1092	+	CT1068-MQG-1076
CT1068-R	TTCGTACACATCACCATTcTaTTaGAAGCTTATGGCAGGC		−	
CT1260-F	GAATGTAGTGGTGCAAATGTgATaaGAGATGTACACAGGCACC	1242–1284	+	CT1260-MQG-1076
CT1260-R	GGTGCCTGTGTACATCTCttATcACATTTGCACCACTACATTC		−	
CT1583-R	CAAAGGGAGAATTCCAACGTATTGGAATCTGGTTcaAGGTTa AAGCGGCACGTTGATGCC	1567–1626	−	CT1583-MQG-1076
CT-F	ACTTTTCTTGGATCTATATCG	250–270	+	
CT-R	CGTCAGCCAATGACCCGAAG	1713–1732	−	
attB2TX30SXN	GGGGACCACTTTGTACAAGAAAGCTGGGTCCTAGACTAGTTCTAG ATCGCGAGCGGCCGCCCTTTTTTTTTTTTTTTTTTTTTTTTTTTT	End	−	

The bold upper case represents the native Mc114 sequence relative to the VP1 start, the upper case represents the gateway primer nucleotides, and the lower case represents the inserted nucleotides to create start or stop codons

Japan). Total RNA (500 ng) from each construct was loaded onto a 2% denaturing agarose gel containing formaldehyde and then transferred to a positively charged nylon transfer membrane (Hybond-N+; Amersham Biosciences, Ireland) under vacuum (VacuGene XL; Pharamacia LKB, Sweden). Northern blotting was carried out according to the DIG Northern Starter Kit (Roche, USA) with an RNA probe corresponding to Mc114 VP1 position 157 to 1283 [9].

Results

Transcription and expression experiments were run in parallel. Northern blot analysis confirmed that rVP1 mRNA, with approximately 2600 nucleotides, was transcribed from all constructs (data not shown). The culture medium was harvested 5–6 dpi and examined for rVP1 expression by Western blotting, using hyperimmune rabbit antisera raised against Mc114 VLPs and *E. coli*-expressed N- and C-terminal VP1 [8]. The predicted VP1 (1683 nt) encoded 561 amino acids with an apparent molecular weight of 60,000 (60 K protein), whereas the predicted N- and C-terminal-deleted rVP1 construct sizes are shown in Fig. 1. The *E. coli*-expressed N-terminal VP1 included nucleotides 1–687, and the *E. coli*-expressed C-terminal VP1 included nucleotides 688–1683. All constructs expressed bands of their predicted sizes as determined by Western blot analysis using different kinds of antisera.

All of the N-terminal-deleted rVP1 constructs were reactive with the *E. coli*-expressed C-terminal VP1 antiserum (Fig. 2A, lanes 1 to 4), whereas the NT49 constructs were reactive with the VLP and *E. coli*-expressed N-terminal VP1

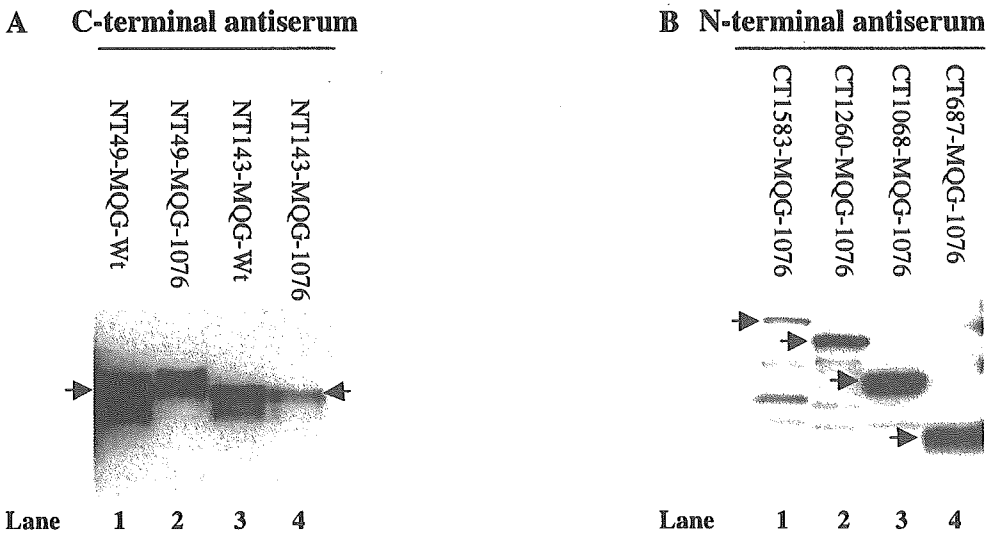

Fig. 2. A Western blot analysis of the cell culture medium for NT49-Wt, NT49-MQG-1076, NT143-Wt, and NT143-MQG-1076 against *E. coli*-expressed C-terminal antiserum (*1* to *4*, respectively) and **B** CT1583-MQG-1076, CT1260-MQG-1076, CT1068-MQG-1076, and CT687-MQG-1076 against *E. coli*-expressed N-terminal antiserum (*1* to *4*). The arrows correspond to the expressed rVP1 for each of the constructs

antisera, and the NT143-Wt was reactive with the VLP antiserum (data not shown). The reason the NT143 constructs were non-reactive with the N-terminal antiserum may be that the antiserum was raised against a region in the deleted VP1 region (i.e., nt 1 to 143), though direct evidence is lacking. All of the C-terminal-deleted rVP1 constructs were reactive with the *E. coli*-expressed N-terminal VP1 antiserum (Fig. 2B, lanes 1 to 4). Not surprisingly, the CT687-MQG-1076 construct was non-reactive with the *E. coli*-expressed C-terminal VP1 antiserum (i.e., the C-terminal VP1 antiserum was raised against a region in the deleted region), whereas the other C-terminal-deleted rVP1 constructs were reactive (data not shown). The CT1583-MQG-1076 was non-reactive with the VLP antiserum, whereas the other three C-terminal-deleted rVP1 constructs were reactive (data not shown). The reason both NT143-MQG-1076 and CT1583-MQG-1076 rVP1 were non-reactive against the VLP antiserum has not yet been determined; however, the Western blot results showed that NT143-MQG-1076 and CT1583-MQG-1076 rVP1 reacted only weakly against the antisera (Fig. 2). Taken as a whole, our results showed that SaV rVP1 was expressed for all deleted N- and C-terminal-deleted rVP1 constructs.

The 5–6 dpi harvested culture medium described above was then examined for VLP formation by negative-stain EM. Despite examining more than 10 grid squares per sample, we found that only the NT49 constructs formed VLPs with

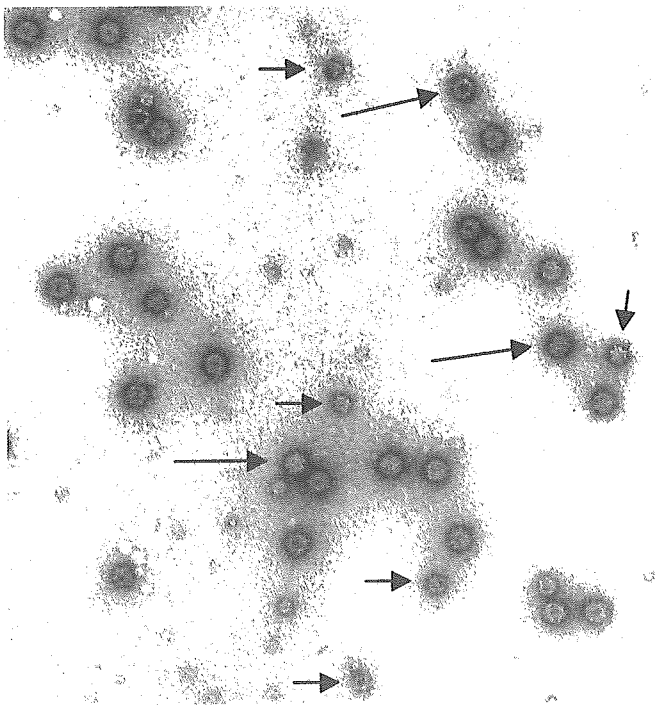

Fig. 3. Electron-microscopic image of CsCl purified Mc114 NT49-MQG-1076 showing both small and native-size VLPs negative-stained with 4% uranyl acetate (pH 4). The long arrows show the native-size VLPs, and short arrows show the small VLPs. The bar indicates 100 nm

morphological features similar to native SaV, having diameters 41–48 nm and the Star of David structure (Fig. 3). However, smaller VLPs were also observed for these NT49 constructs, having approximately 26–31 nm diameters and spikes on the outline (Fig. 3). These small VLPs appeared to have similar morphological features to small SaV GV VLPs, which also had spikes on the outline [10].

We further investigated the NT49-MQG-1076 construct by infecting NT49-MQG-1076 recombinant baculoviruses to approximately 2×10^8 confluent Tn5 cells and incubating them for 6 days. The VLPs were purified by CsCl equilibrium gradient ultracentrifugation as previously described [7]. Twelve fractions were collected, and a 58 K band was detected in fractions 7 and 8 by Western blotting (Fig. 4A). This result was confirmed by our previously described ELISA (Fig. 4B) [10]. By EM, fractions 7, 8, 9, and 10 were found to contain both small and native-size VLPs. The amino acid sequence of the 58 K band of fraction 7 was determined using Edman's degradation method and was found to be MVVDP,

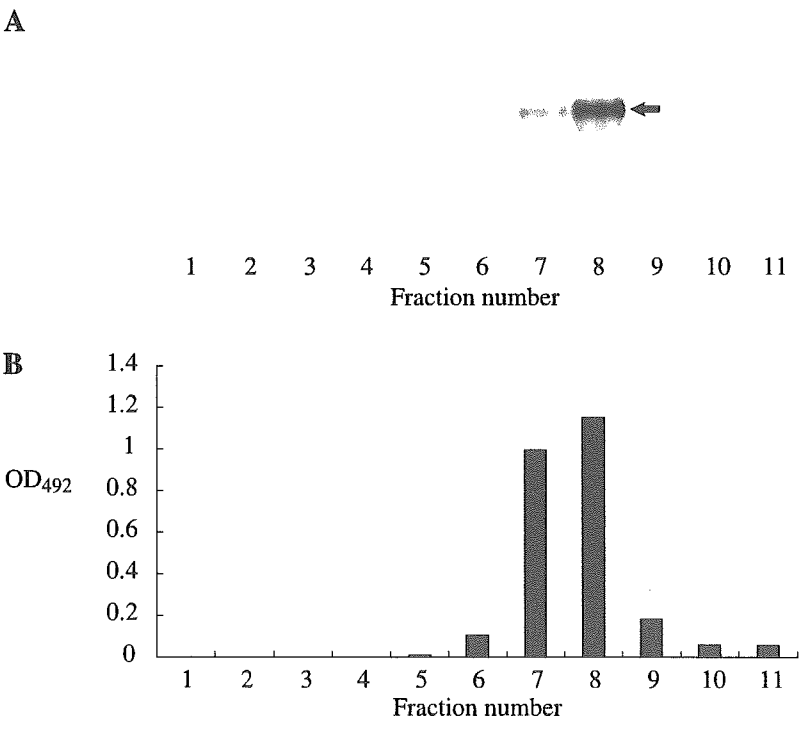

Fig. 4. The NT49-MQG-1076 recombinant baculoviruses were infected to approximately 2×10^8 confluent Tn5 cells and incubated for 6 days. The VLPs were purified by CsCl equilibrium gradient ultracentrifugation, and 12 fractions were collected. **A** Western blotting (*E. coli*-expressed C-terminal antiserum) showed that NT49-MQG-1076 rVP1 (58 K) was present in fractions 7 and 8 (arrow), and **B** an antigen ELISA, which used hyperimmune rabbit (capture) and guinea pig (detector) antiserum raised against MQG-1076 VLPs, showed that VLPs were present in fractions 6 to 11, though the majority of VLPs were in fractions 7 and 8

which matched the NT49 construct start sequence. Interestingly, the position of this second methionine was maintained in SaV GV strains [9], whereas for SaV GII, GIII, and GIV strains a second methionine residue was located further downstream. Our results suggest that the formation of these smaller VLPs was probably controlled by the first 48 nucleotides of VP1. The numbers of the small SaV VLPs appeared to be much lower than those of the native-size VLPs. Our results suggested that SaV small VLPs were unstable, since they appeared to lose their morphological features when stored at 4 °C for several months (data not shown). Likewise in a NoV expression study, small NoV VLPs were reported to be less stable than native-size NoV VLPs [12].

Discussion

Our expression results were similar to those reported in a RHDV N- and C-terminal-deleted rVP1 expression study [1]. The formation of small RHDV VLPs was not observed with a construct that deleted 103 amino acids of the N-terminal region, but it was observed with constructs that deleted either 29 or 61 amino acids of the N-terminal region. These results suggested that the 29 amino acids at the N-terminal region played a crucial role in the formation of small and native-size VLPs. Our results clearly indicated that at least the first 16 amino acids at the N-terminal region played a crucial role in the formation of SaV VLPs. In comparison, SaV and RHDV N-terminal regions, 16 and 29 amino acids, respectively, shared only the first three amino acids, MEG. The MEG capsid start motif is conserved among all human SaV strains, whereas human NoV strains do not contain this sequence. However, porcine SaV, which belongs to GIII, does not contain this motif, though small porcine VLPs have yet to be reported. Further investigations with other human SaV genogroups are needed to help define the sequences that control the formation of the SaV VLPs.

The formation of these smaller SaV GI VLPs was observed only when the first 48 nucleotides of VP1 were deleted, whereas the formation of smaller SaV GV VLPs was observed using a construct that began from the predicted start codon [10]. Small SaV virions have not yet been described in clinical stool specimens, which may suggest that these smaller VLPs were exclusive to insect cell expression. However, since these smaller VLPs lacked native SaV morphological features, identification may be difficult in clinical specimens.

Classification of caliciviruses has been hampered mostly because many caliciviruses cannot be grown in cell culture [6]. In the early 1980s, caliciviruses were grouped based on morphological features [4], but as sequence data accumulated in the 1990s, the International Committee on Taxonomy of Viruses (ICTV) created four genera in the family *Caliciviridae*, primarily based on phylogenetic analysis. On the other hand, Green et al. [6] mentioned that proteolytic processing and differences in the replication strategy may also be important tools for distinguishing caliciviruses. In this study we expressed SaV N- and C-terminal-deleted rVP1 constructs in a baculovirus expression system. All constructs transcribed rVP1 mRNA and expressed rVP1, but VLP formation was only observed with

N-terminal-deleted rVP1 constructs (NT49-Wt and NT49-MQG-1076 constructs). Of novel findings was the formation of smaller and native-size VLPs for these two SaV N-terminal-deleted rVP1 constructs. These results were similar to those reported in a RHDV N- and C-terminal-deleted rVP1 expression study [1] but were distinct from those reported in a NoV N- and C-terminal-deleted rVP1 expression study [2]. Barcena et al. [1] showed that RHDV N-terminal-deleted rVP1 constructs could form small and native-size VLPs and that all RHDV C-terminal-deleted rVP1 constructs failed to form VLPs, whereas Bertolotti-Ciarlet et al. [2] showed that both NoV N- and C-terminal-deleted rVP1 constructs could form VLPs. It is tempting to draw parallels for these studies and propose that SaV expression was more closely related to RHDV than to expression of NoV in insect cells. What's more, SaV and RHDV strains have a similar genomic organization, and their small and native-size VLPs appeared to have similar morphological features, hinting that these two genera may have evolved from a common ancestor.

Acknowledgements

This work was supported by Grants-in-aid from The Ministry of Education, Culture, Sports, Science and Technology, Japan, and a Grant for Research on Re-emerging Infectious Diseases from The Ministry of Health, Labour, and Welfare, Japan. We are grateful to the Japanese Monbusho for the PhD scholarship provided to Grant Hansman.

References

1. Barcena J, Verdaguer N, Roca R, Morales M, Angulo I, Risco C, Carrascosa JL, Torres JM, Caston JR (2004) The coat protein of rabbit hemorrhagic disease virus contains a molecular switch at the N-terminal region facing the inner surface of the capsid. Virology 322: 118–134
2. Bertolotti-Ciarlet A, White LJ, Chen R, Prasad BV, Estes MK (2002) Structural requirements for the assembly of Norwalk virus-like particles. J Virol 76: 4044–4055
3. Bertolotti-Ciarlet A, Crawford SE, Hutson AM, Estes MK (2003) The 3′ end of Norwalk virus mRNA contains determinants that regulate the expression and stability of the viral capsid protein VP1: a novel function for the VP2 protein. J Virol 77: 11603–11615
4. Caul EO, Appleton H (1982) The electron microscopical and physical characteristics of small round human fecal viruses: an interim scheme for classification. J Med Virol 9: 257–265
5. Chen R, Neill JD, Noel JS, Hutson AM, Glass RI, Estes MK, Prasad BV (2004) Inter- and intragenus structural variations in caliciviruses and their functional implications. J Virol 78: 6469–6479
6. Green KY, Ando T, Balayan MS, Berke T, Clarke IN, Estes MK, Matson DO, Nakata S, Neill JD, Studdert MJ, Thiel HJ (2000) Taxonomy of the caliciviruses. J Infect Dis 181 [Suppl 2]: S322–S330
7. Hansman G, Doan LP, Kguyen T, Okitsu S, Katayama K, Ogawa S, Natori K, Takeda N, Kato Y, Nishio O, Noda M, Ushijima H (2004) Detection of norovirus and sapovirus infection among children with gastroenteritis in Ho Chi Minh City, Vietnam. Arch Virol 149: 1673–1688
8. Hansman GS, Katayama K, Maneekarn N, Peerakome S, Khamrin P, Tonusin S, Okitsu S, Nishio O, Takeda N, Ushijima H (2004) Genetic diversity of norovirus and sapovirus in

hospitalized infants with sporadic cases of acute gastroenteritis in Chiang Mai, Thailand. J Clin Microbiol 42: 1305–1307
9. Hansman GS, Katayama K, Oka T, Natori K, Takeda N (2005) Mutational study of sapovirus expression in insect cells. Virol J 2: 13
10. Hansman GS, Natori K, Oka T, Ogawa S, Tanaka K, Nagata N, Ushijima H, Takeda N, Katayama K (2005) Cross-reactivity among sapovirus recombinant capsid proteins. Arch Virol 150: 21–36
11. Prasad BV, Hardy ME, Dokland T, Bella J, Rossmann MG, Estes MK (1999) X-ray crystallographic structure of the Norwalk virus capsid. Science 286: 287–290
12. White LJ, Hardy ME, Estes MK (1997) Biochemical characterization of a smaller form of recombinant Norwalk virus capsids assembled in insect cells. J Virol 71: 8066–8072

Author's address: Dr. Grant S. Hansman, Department of Virology II, National Institute of Infectious Diseases, 4-7-1 Gakuen, Musashimurayama, Tokyo, 208-0011, Japan; e-mail: ghansman@nih.go.jp

Arch Virol (2005) 150: 2539–2548
DOI 10.1007/s00705-005-0591-0

Archives of Virology
Printed in Austria

Cleavage activity of the sapovirus 3C-like protease in *Escherichia coli*

T. Oka, K. Katayama, S. Ogawa, G. S. Hansman, T. Kageyama, T. Miyamura, and N. Takeda

Department of Virology II, National Institute of Infectious Diseases, Tokyo, Japan

Received March 22, 2005; accepted May 19, 2005
Published online August 1, 2005

Summary. We recently determined the ORF1 cleavage map of Mc10, a human sapovirus (SaV) strain, as follows: NH_2–p11-p28-p35(NTPase)-p32-p14(VPg)-p70(Pro-Pol)-p60(VP1)–COOH. This cleavage was dependent on the viral encoded 3C-like protease. To identify the cleavage site of SaV ORF1, putative p70 (Pro-Pol) and p14-p70 (VPg-Pro-Pol) were expressed as N-terminal GST and C-terminal 6 × His-tag fusion proteins in *Escherichia coli*, and the expressed products were analyzed by SDS-PAGE and Western blotting. Our results indicated that the efficient proteolytic cleavage occurred between p14 (VPg) and p70 (Pro-Pol), and N-terminal amino acid sequencing revealed that the cleavage site was between E^{1055} and A^{1056}. In contrast, the p70 (Pro-Pol) was not further cleaved. We also found that SaV protease cleaved the Q/G site within the rhinovirus 3C protease recognition site. Site-directed mutagenesis in a conserved GDCG motif of the protease completely abolished these proteolytic activities. This is the first report to identify the cleavage site of the SaV ORF1 polyprotein.

Introduction

Sapovirus (SaV), a member the family *Caliciviridae*, is a causative agent of human and porcine gastroenteritis [9, 12, 18]. SaV strains are currently divided into five genetic groups, genogroups I (GI) to GV, of which the GI, GII, GIV, and GV strains infect humans [6]. Although GIII porcine SaV is able to grow in cultured cells, there have been no studies in which SaV was cultured in human cells, and no animal model of human SaV has been developed [3]. The SaV genome is a positive-sense, single-strand RNA molecule of approximately 7.5 kb that is polyadenylated at its 3′ terminus. The genome of the SaV GI, GIV, and GV strains are predicted to contain three main open reading frames (ORFs), whereas those of SaV GII and

GIII strains have two ORFs [6, 8, 15, 20, 22–24]. The SaV ORF1 encodes non-structural proteins and the capsid protein (VP1), whereas ORF2 and ORF3 encode proteins of as-yet-unknown function [5]. The SaV ORF1 polyprotein contains amino acid (aa) motifs conserved in 2C-like NTPase (NTPase), VPg, 3C-like protease (Pro), 3D-like RNA-dependent RNA polymerase (Pol), and capsid protein (VP1) of caliciviruses [5].

Our previous study of a SaV GII strain, Mc10, demonstrated that the ORF1 polyprotein is processed into at least 10 major proteins, p11, p28, p35, p32, p14, p70, p60, p66, p46, and p120. Seven of these products were arranged in the following order: NH_2–p11-p28-p35(NTPase)-p32-p14(VPg)-p70(Pro-Pol)-p60(VP1)–COOH [21].

Mutagenesis of the GDCG motif in the 3C-like protease fully abolished the proteolytic activity, demonstrating that the cleavage was dependent on viral encoded 3C-like protease [21]. Although p70 (Pro-Pol) has two aa motifs characteristic of Pro and Pol, we were unable to demonstrate further processing in an *in vitro* rabbit reticulocyte-coupled transcription-translation system [21]. Inefficient cleavage of the protein corresponding to p70 has also been reported in other caliciviruses, including Norovirus (NoV), rabbit hemorrhagic disease virus (RHDV), and feline calicivirus (FCV), when a similar *in vitro* system was used [1, 17, 27, 28, 31]. In contrast, further cleavage between Pro and Pol was demonstrated when the Pro-containing regions derived from RHDV, NoV, and FCV were expressed in *Escherichia coli* (*E. coli*) [2, 16, 17, 25–28, 30].

The objective of this study was to determine whether the putative p70 (Pro-Pol) region of human SaV is further cleaved in *E. coli*. We also aimed to identify the cleavage site around the protease domain, because none of the cleavage sites in the SaV ORF1 have been identified.

Materials and methods

Virus and full-length cDNA clones

SaV GII Mc10 strain (Hu/SaV/Mc10/2000/Thailand; GenBank accession number AY237420) was isolated from an infant hospitalized with acute gastroenteritis in Chiang Mai, Thailand, in 2000 [10]. Two clones constructed previously [21] were used as a template for PCR. The first clone, pUC19/SaV Mc10 full-length, contained the native Mc10 sequence. The second clone, pUC19/SaV full-C1171A/ORF1, was a protease mutant and has nucleotide changes from TGT (^{1171}C) to GCG (^{1171}A) in the GDCG motif.

Construction of E. coli expression plasmids

Putative p70 (Pro-Pol) and p14-p70 (VPg-Pro-Pol) derived from Mc10 (Fig. 1) were selected for the expression in *E. coli*. A DNA fragment corresponding to either p70 (nt 3179–5173, aa 1056–1720) or p14-p70 (nt 2834–5173, aa 941–1720) with or without nucleotide changes from TGT (^{1171}C) to GCG (^{1171}A) in the GDCG motif was amplified by a sense primer including a *Bam*HI site for p70, (5′-CAGGGGCCCCTGGGATCCgctcccacaccaattgtt acattc-3′); for p14-p70, (5′-CAGGGGCCCCTGGGATCCgccaaaggaaagaccaagcatggc-3′; the *Bam*HI site is underlined) and an antisense primer (5′-GCCGCTCGAGTCGACTCA GTGATGGTGATGGTGATGttcaaacactaatttggtggtctcttcactggggct-3′) including a 6 × His-

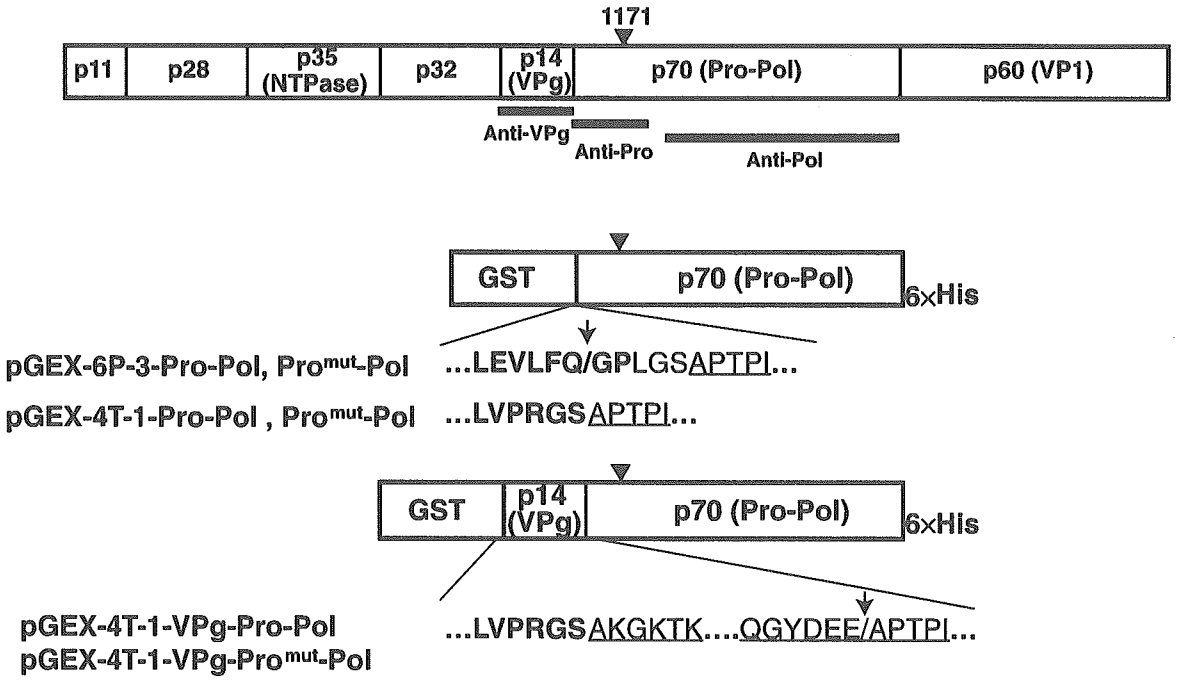

Fig. 1. Cleavage map of Mc10 ORF1 and the construction of the expression plasmids. Schematic representation of the fusion proteins expressed in *E. coli*. Putative p70 (Pro-Pol) was cloned into pGEX-6P-3 and pGEX-4T-1 vectors, and putative p14-p70 (VPg-Pro-Pol) was cloned into a pGEX-4T-1 vector. Closed triangles indicate the position in the 3C-like protease where the ^{1171}C-to-^{1171}A change was introduced. Both the wild and mutant (Pro^{mut}) forms of the constructs were used for the expression. The recombinant proteins were expressed as the N-terminal GST and C-terminal 6 × His- tag fusion proteins. The protease recognition sites derived from the vectors are indicated in bold and the SaV sequences are underlined. The cleavage sites identified in this study are indicated by slashes and arrows

tag sequence (double-underlined), a stop codon (bold), and a *Sal*I site (underlined). PCR was performed with 500 ng of each full-length cDNA.

The PCR products were purified and digested with *Bam*HI and *Sal*I (New England Biolabs, Beverly, MA) and cloned into the corresponding sites of either pGEX-6P-3 or pGEX-4T-1 vectors (Amersham Biosciences, Piscataway, NJ). *E. coli* DH5α cells (Toyobo, Osaka, Japan) were used for the transformation and propagation of the plasmids. All plasmids were verified by sequence analysis. Six plasmids containing putative p70 (Pro-Pol) or p14-p70 (VPg-Pro-Pol) sequences were prepared and were designated as pGEX-6P-3- Pro-Pol, pGEX-6P-3-Pro^{mut}-Pol, pGEX-4T-1-Pro-Pol, pGEX-4T-1-Pro^{mut}-Pol, pGEX-4T-1-VPg-Pro-Pol, and pGEX-4T-1-VPg-Pro^{mut}-Pol (Fig. 1). The designation "Pro^{mut}" refers to a protease in which C was changed to A in the GDCG motif, as described previously [21].

Expression of recombinant proteins in E. coli

The products were expressed as fusion proteins with glutathione S-transferase (GST) at the N-terminus and 6 × His-tag at the C-terminus. *E. coli* BL21-CodonPlus-RIL cells (Stratagene, La Jolla, CA) were transformed with the expression plasmids, and the transformants were incubated at 37 °C in 10 ml of Luria Broth containing 50 μg/ml of ampicillin and 50 μg/ml

of chloramphenicol until the OD_{600} value reached 0.6–0.8. The expression was induced in a final concentration of 1 mM isopropyl-1-thio-β-D-galactopyranoside followed by incubation at 37 °C for 3 h.

Analysis of recombinant proteins

The *E. coli* culture or purified recombinant proteins were mixed with an equal volume of the 2 × SDS-PAGE sample buffer (125 mM Tris-HCl (pH 6.8), 10% (w/v) sucrose, 4% (w/v) SDS, and 0.004% (w/v) bromophenol blue with 10% (v/v) 2-mercaptoethanol), and heated at 95 °C for 5 min prior to loading on 5–20% Tris-Glycine polyacrylamide gel (ATTO, Tokyo, Japan). Electrophoresis was performed in 25 mM Tris/192 mM glycine/0.1% SDS buffer at 20 mA for 1.5 h. The proteins in the gel were visualized by staining with GelCode Blue Staining Reagent (Pierce, Rockford, IL). Precision Plus Protein All Blue standards (BioRad, Hercules, CA) were used as a size marker for CBB staining and Magicmark XP Western standard (Invitrogen, Carlsbad, CA) was used as a size marker for the Western blotting.

For Western blotting, the proteins separated in the gel were electrically blotted onto a PVDF membrane (Immobilon-P; Millipore, Billerica, MA) and detected with anti-His tag monoclonal antibodies (Roche Diagnostics, Tokyo, Japan) at a dilution of 1:500, horseradish peroxidase-conjugated anti-GST goat-polyclonal antibody (Amersham Biosciences) at a dilution of 1:5000, or anti-VPg, -Pro, -Pol rabbit hyperimmune IgG (Fig. 1) at a dilution of 1:3000 as previously described [11, 21]. The membrane was treated with ECL detection reagent (Amersham Biosciences) according to the manufacturer's instructions, and the signals were exposed on film (Fuji Film, Tokyo, Japan).

The recombinant proteins were purified using TALON resin (BD Clontech, Palo Alto, CA) as previously described [21], then subjected to N-terminal amino acid sequencing (APRO Science, Tokushima, Japan).

Results

Analysis of Pro-Pol recombinant proteins

To determine whether the p70 (Pro-Pol) of human SaV (Fig. 1) is further cleaved in *E. coli*, putative p70 (Pro-Pol) was expressed as a fusion protein using an *E. coli* expression plasmid, pGEX-6P-3-Pro-Pol. The recombinant protein contains GST at the N-terminus and 6 × His-tag at the C-terminus. Three major products of approximately 96, 70, and 26 kDa were visualized when the total lysate was analyzed by SDS-PAGE (Fig. 2A, lane 1). Western blot analysis revealed that the 96 kDa protein was immunoreactive to anti-GST, anti-His tag, anti-Pro, and anti-Pol antibodies (lane 1 in Fig. 2B, C, E, and F), and thus corresponds to the GST-Pro-Pol-6 × His fusion protein. The 26 kDa band corresponds to GST, because it was solely detected by anti-GST (Fig. 2B, lane 1), whereas the 70 kDa band corresponds to Pro-Pol-6 × His, as it was detected by anti-Pro, anti-Pol, and anti-His tag antibodies (lane 1 in Fig. 2C, E, and F). These results indicated that the cleavage between Pro and Pol did not occur in *E. coli* as observed in our previous study with an *in vitro* transcription/translation system [21].

To identify the cleavage site between the 26 kDa and 70 kDa proteins, the N-terminal amino acid sequence of the affinity-purified 70 kDa protein was determined. The amino acid sequence was G (7.6 pmol)-P (6.2 pmol)-L (7.7 pmol)-G

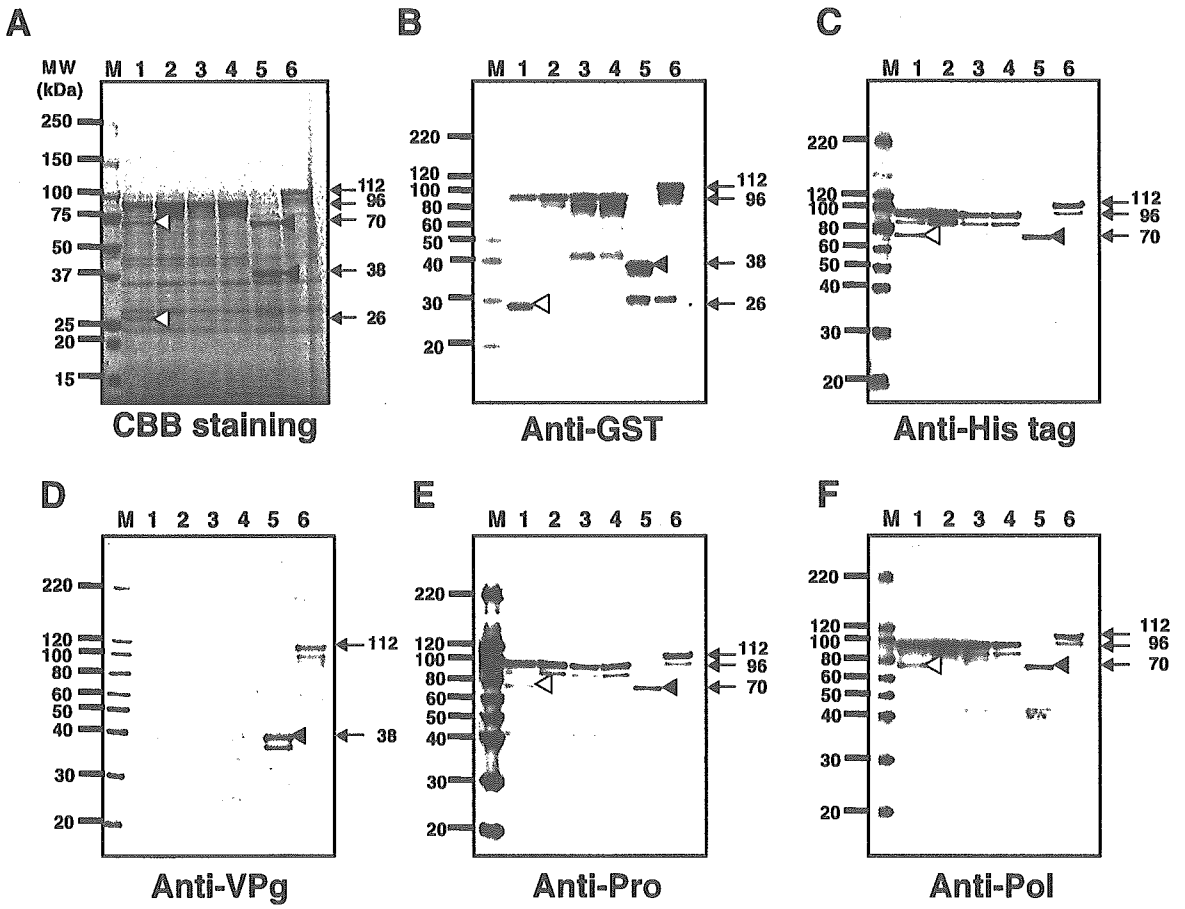

Fig. 2. Analysis of the products expressed in *E. coli.* A Coomassie brilliant blue (CBB) staining. Western blot analysis with B anti-GST antibody, C anti-His tag antibody, D anti-VPg antibody (raised against aa 941–1055), E anti-Pro antibody (raised against aa 1056–1194), and F anti-Pol antibody (raised against aa 1247–1720). Lane *M* indicates the molecular size marker. *1*, pGEX-6P-3-Pro-Pol; *2*, pGEX-6P-3-Pro^{mut}-Pol; *3*, pGEX-4T-1-Pro-Pol; *4*, pGEX-4T-1-Pro^{mut}-Pol; *5*, pGEX-4T-1-VPg-Pro-Pol; *6*, pGEX-4T-1-VPg-Pro^{mut}-Pol. The products of interest are indicated by arrows on the right side of the gel. The specific cleavage products derived from pGEX-6P-3-Pro-Pol, and those from pGEX-4T-1-VPg-Pro-Pol are indicated by open and closed triangles, respectively. Anti-VPg, anti-Pro, and anti-Pol antibodies are designated as Anti-D, E, and F, respectively [21]

(7.7 pmol)-S (1.8 pmol), which is not encoded in the SaV p70 (Pro-Pol) sequence (Fig. 1). Because the original plasmid, pGEX-6P-3, used for the expression study contains a human rhinovirus 3C protease recognition sequence (LEVLFQGP) plus a sequence derived from a multi-cloning site of the vector (LGS) between GST and putative Pro-Pol (APTPI. . .), as depicted in Fig. 1, the Q/G site within the human rhinovirus 3C protease recognition sequence was recognized by SaV 3C-like protease, and generated two major products of 26 kDa (GST-LEVLFQ)

and 70 kDa (GPLGS-Pro-Pol-6 × His), though the cleavage site did not originate from the native SaV sequence.

To demonstrate that proteolytic cleavage was mediated by SaV protease, a plasmid containing a mutated protease, pGEX-6P-3-Pro^{mut}-Pol, was constructed and the proteins were expressed in *E. coli*. A major fusion protein with an apparent molecular mass of 96 kDa was observed (Fig. 2A, lane 2). This protein was immunoreactive with anti-GST, anti-His tag, anti-Pro, and anti-Pol antibodies (Lane 2 in Fig. 2B, C, E, and F), indicating that C1171A mutation in the SaV protease abolished the cleavage activity at the Q/G site within the human rhinovirus 3C protease recognition sequence. The finding that C^{1171} played a critical role in the protease activity was consistent with our previous observation made using an *in vitro* coupled transcription-translation system [21].

To further confirm the specificity of the SaV 3C-like protease, the putative p70 (Pro-Pol) region that contained either the wild-type or C1171A mutant (designated as Pro^{mut}) was cloned into the pGEX-4T-1 vector, which contained a thrombin recognition sequence (LVPRGS) at the C-terminus of the GST. The recombinant protein should be GST-LVRGS-p70 (APTPI...)-6 × His, as depicted in Fig. 1. When the pGEX-4T-1-Pro-Pol and pGEX-4T-1-Pro^{mut}-Pol were expressed in *E. coli*, a major fusion protein with an apparent molecular mass of 96 kDa was observed in both lysates (Fig. 2A, lanes 3 and 4). Western blot analysis revealed that these products were immunoreactive to anti-GST, anti-His tag, anti-Pro, and anti-Pol antibodies (Fig. 2B, C, E, and F, lanes 3 and 4), indicating that the fusion protein was GST-Pro-Pol-6 × His.

We detected smaller products by Western blot analyses (Fig. 2B, C, E, and F, lanes 1, 2, 3, and 4) and these were likely to be N-terminal truncated forms of the fusion protein – i.e., they were likely to have been cleaved by *E. coli* proteases, because of the reactivity against a set of the antibodies.

These results indicated the following: (i) there is no cleavage between Pro and Pol; (ii) the Q/G site within the human rhinovirus 3C protease recognition sequence was cleaved by the SaV 3C-like protease; and (iii) C^{1171} was critical for the cleavage activity.

Analysis of the VPg-Pro-Pol recombinant proteins

To determine whether the cleavage occurs between VPg and Pro-Pol, both the wild and Pro^{mut} forms of the putative p14-p70 sequence (VPg-Pro-Pol) were expressed as an N-terminal GST and a C-terminal 6 × His-tag fusion protein. The recombinant protein should be GST-LVRGS-VPg(AKGKTK...)-Pro-Pol-6 × His, as depicted in Fig. 1.

When the total lysate of *E. coli* cells harboring pGEX-4T-1-VPg-Pro-Pol was analyzed by SDS-PAGE, two major proteins of approximately 38 kDa and 70 kDa were visualized (Fig. 2A, lane 5). Western blot analysis revealed that the 38 kDa protein corresponds to GST-VPg, because it was detected by anti-GST and anti-VPg antibodies (Fig. 2B and D, lane 5), whereas the 70 kDa protein corresponded to Pro-Pol-6 × His, as it was detected by anti-His tag, anti-Pro-,

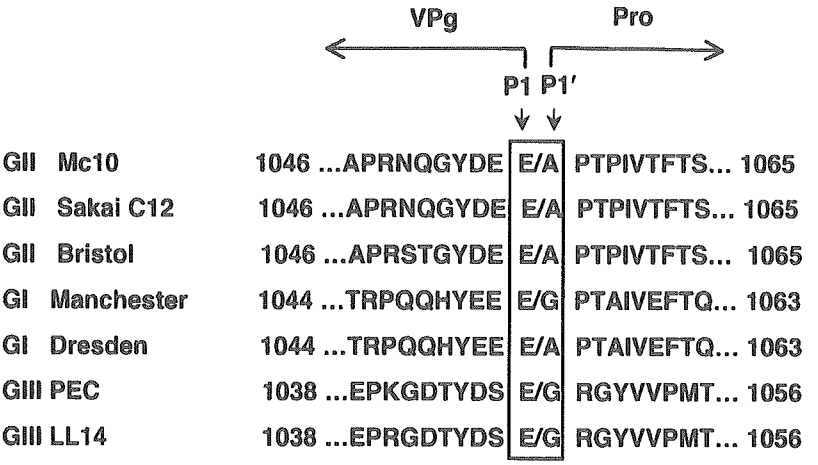

Fig. 3. Comparison of the amino acids sequences of the putative p14 (VPg) and p70 (Pro-Pol) junction of SaV, for which the full-length genomic sequence has been determined. Amino acids at positions P1 and P1′ of the cleavage site of the Mc10, and the corresponding site of the other SaV strains are boxed. The positions of the amino acid residues in the ORF polyprotein are indicated on both sides of the figure. The GenBank accession numbers are as follows: Mc10, AY237420; Sakai C12, AY603425; Bristol, AJ249939; Manchester, X86560; Dresden, AY694184; PEC, AF182760; and LL14, NC_000940

and anti-Pol antibodies (Fig. 2C, E, and F, lane 5). The N-terminal amino acid sequence of the purified 70 kDa protein was A (8.1 pmol)-P (4.8 pmol)-T (3.8 pmol)-P (4.0 pmol)-I (2.8 pmol), which corresponds to SaV Mc10 ORF1 aa 1056–1060 (Fig. 3). These results indicated that the efficient cleavage occurred between E^{1055} and A^{1056}, which is the exact predicted boundary site between the p14 (VPg) and p70 (Pro-Pol). A major product with a predicted size of 112 kDa was observed when the pGEX-4T-1-VPg-Pro^{mut}-Pol plasmid was expressed. This product was immunoreactive to anti-GST, anti-His tag, anti-VPg, anti-Pro, and anti-Pol antibodies (Fig. 2A–F, lane 6), demonstrating that the cleavage was dependent on the SaV protease activity.

We also detected smaller products by Western blot analyses (lane 5 in Fig. 2B and D, lane 6 in 2B, 2C, 2D, 2E, and 2F). These appeared to be N-terminal truncated forms of the fusion proteins, and were not examined further.

The results indicated the following: (i) efficient cleavage occurred between E^{1055} and A^{1056}, at the exact predicted boundary site between the p14 (VPg) and p70 (Pro-Pol); and (ii) C^{1171} was critical for this cleavage activity.

Discussion

Cleavage between Pro and Pol has been reported in other members of caliciviruses in studies using recombinant proteins expressed in *E. coli* [2, 16, 17, 25–28, 30]. In this study, however, we did not detect the viral protein corresponding to the Pro and Pol. Prolonged expression in *E. coli*, i.e., up to 16 h, also failed to identify further

cleavage product(s) (data not shown). It has been demonstrated that the Pro-Pol precursor accumulated in RHDV-infected hepatocytes and also in FCV-infected cells [7, 13, 28]. Furthermore, a 70 kDa protein corresponding to Pro-Pol was recently identified in porcine enteric calicivirus (PEC: SaV GIII strain)-infected LLC-PK cells [4]. The lack of the cleavage in the Pro-Pol suggested that SaV p70 has both protease and polymerase activities as previously reported in the case of FCV [14, 29].

The residues E (or Q)/G, A, S, T, D, N have been identified as the cleavage sites in other caliciviruses [1, 19, 25, 27]. In this study, we demonstrated that the SaV protease cleaves between E^{1055} and A^{1056}, at the exact predicted boundary site between the p14 (VPg) and p70 (Pro-Pol). We also found that the SaV 3C-like protease cleaves the Q/G site within the rhinovirus 3C protease recognition sequence as reported in the Chiba virus, in the genus *Norovirus* [25]. Although the cleavage efficiency was significantly different between GST-p14-p70 and GST-p70, it may depend on either vector- or virus-derived sequence. Nevertheless, these characteristics were consistent with those of other calicivirus 3C-like proteases, in which the cleavage occurs after either glutamic acid (E) or glutamine (Q).

Identification of the N-terminal sequence of the p70 (Pro-Pol) demonstrated that our prediction of the boundary between p14 (VPg) and p70 (Pro-Pol) was correct. To date, seven SaV complete genomes belonging to GI, GII, and GIII have been reported. When the amino acid sequences surrounding the E^{1055}/A^{1056} site were aligned, the amino acid E in the P1 and G (or A) in the P1′ position (P1 is the amino acid immediately upstream of the scissile bond, and P1′ is the amino acid immediately downstream of the scissile bond) were commonly conserved among SaV strains (Fig. 3). Although we found several EA and QG sequences within the putative p14-p70 region, these were not cleaved by the SaV protease. Interestingly, these sites were not conserved among SaV strains (data not shown), suggesting that other cleavage sites in the SaV ORF1 polyprotein would be conserved among the SaV strains. Further studies are needed to identify other cleavage sites to confirm this expectation.

Acknowledgements

This work was supported in part by a grant for Research on Emerging and Re-emerging Infectious Diseases from the Ministry of Health, Labor and Welfare of Japan.

References

1. Belliot G, Sosnovtsev SV, Mitra T, Hammer C, Garfield M, Green KY (2003) In vitro proteolytic processing of the MD145 norovirus ORF1 nonstructural polyprotein yields stable precursors and products similar to those detected in calicivirus-infected cells. J Virol 77: 10957–10974
2. Blakeney SJ, Cahill A, Reilly PA (2003) Processing of Norwalk virus nonstructural proteins by a 3C-like cysteine proteinase. Virology 308: 216–224
3. Chang KO, Sosnovtsev SV, Belliot G, Kim Y, Saif LJ, Green KY (2004) Bile acids are essential for porcine enteric calicivirus replication in association with down-regulation

of signal transducer and activator of transcription 1. Proc Natl Acad Sci USA 101: 8733–8738
4. Chang KO, Sosnovtsev SS, Belliot G, Wang Q, Saif LJ, Green KY (2005) Reverse genetics system for porcine enteric calicivirus, a prototype sapovirus in the caliciviridae. J Virol 79: 1409–1416
5. Clarke IN, Lambden PR (2000) Organization and expression of calicivirus genes. J Infect Dis 181[Suppl 2]: S309–S316
6. Farkas T, Zhong WM, Jing Y, Huang PW, Espinosa SM, Martinez N, Morrow AL, Ruiz-Palacios GM, Pickering LK, Jiang X (2004) Genetic diversity among sapoviruses. Arch Virol 149: 1309–1323
7. Green KY, Mory A, Fogg MH, Weisberg A, Belliot G, Wagner M, Mitra T, Ehrenfeld E, Cameron CE, Sosnovtsev SV (2002) Isolation of enzymatically active replication complexes from feline calicivirus-infected cells. J Virol 76: 8582–8595
8. Guo M, Chang KO, Hardy ME, Zhang Q, Parwani AV, Saif LJ (1999) Molecular characterization of a porcine enteric calicivirus genetically related to Sapporo-like human caliciviruses. J Virol 73: 9625–9631
9. Guo M, Hayes J, Cho KO, Parwani AV, Lucas LM, Saif LJ (2001) Comparative pathogenesis of tissue culture-adapted and wild-type Cowden porcine enteric calicivirus (PEC) in gnotobiotic pigs and induction of diarrhea by intravenous inoculation of wild-type PEC. J Virol 75: 9239–9251
10. Hansman GS, Katayama K, Maneekarn N, Peerakome S, Khamrin P, Tonusin S, Okitsu S, Nishio O, Takeda N, Ushijima H (2004) Genetic diversity of norovirus and sapovirus in hospitalized infants with sporadic cases of acute gastroenteritis in Chiang Mai, Thailand. J Clin Microbiol 42: 1305–1307
11. Hansman GS, Natori K, Oka T, Ogawa S, Tanaka K, Nagata N, Ushijima H, Takeda N, Katayama K (2005) Cross-reactivity among sapovirus recombinant capsid proteins. Arch Virol 150: 21–36
12. Katayama K, Miyoshi T, Uchino K, Oka T, Tanaka T, Takeda N, Hansman GS (2004) Novel recombinant sapovirus. Emerg Infect Dis 10: 1874–1876
13. Konig M, Thiel HJ, Meyers G (1998) Detection of viral proteins after infection of cultured hepatocytes with rabbit hemorrhagic disease virus. J Virol 72: 4492–4497
14. Kuyumcu-Martinez M, Belliot G, Sosnovtsev SV, Chang KO, Green KY, Lloyd RE (2004) Calicivirus 3C-like proteinase inhibits cellular translation by cleavage of poly(A)-binding protein. J Virol 78: 8172–8182
15. Liu BL, Clarke IN, Caul EO, Lambden PR (1995) Human enteric caliciviruses have a unique genome structure and are distinct from the Norwalk-like viruses. Arch Virol 140: 1345–1356
16. Liu BL, Viljoen GJ, Clarke IN, Lambden PR (1999) Identification of further proteolytic cleavage sites in the Southampton calicivirus polyprotein by expression of the viral protease in E. coli. J Gen Virol 80: 291–296
17. Martin Alonso JM, Casais R, Boga JA, Parra F (1996) Processing of rabbit hemorrhagic disease virus polyprotein. J Virol 70: 1261–1265
18. Mayo MA (2002) A summary of taxonomic changes recently approved by ICTV. Arch Virol 147: 1655–1663
19. Meyers G, Wirblich C, Thiel HJ, Thumfart JO (2000) Rabbit hemorrhagic disease virus: genome organization and polyprotein processing of a calicivirus studied after transient expression of cDNA constructs. Virology 276: 349–363
20. Numata K, Hardy ME, Nakata S, Chiba S, Estes MK (1997) Molecular characterization of morphologically typical human calicivirus Sapporo. Arch Virol 142: 1537–1552